

Fluctuating Initial Conditions and Anisotropic Flows

Fernando G. GARDIM^{1,*}, Yojiro HAMA¹ and Frédérique GRASSI¹

¹*Instituto de Física, Universidade de São Paulo, C.P. 66318, 05315-970,
São Paulo-SP, Brazil*

August 19, 2018

Abstract

In this work we study the connection between anisotropic flows and lumpy initial conditions for Au+Au collisions at 200GeV. We present comparisons between anisotropic flow coefficients and eccentricities up to sixth order, and between initial condition reference angles and azimuthal particle distribution angles. We also present a toy model to justify the lack of connection between flow coefficients and eccentricities for individual events.

1 Introduction

The anisotropy in the azimuthal particle distribution in relativistic heavy-ion collisions has been interpreted as an indication of the creation of a strongly interacting Quark-Gluon Plasma (QGP) in the liquid phase with low viscosity. However, this anisotropy should reflect the initial spatial deformation of the matter created. Recently, several analyses have been performed in an effort to understand the relation between anisotropic flows and the initial-conditions (IC) geometry [1, 2], pointing out a close relation between the elliptic flow v_2 and the ellipticity of the IC ε_2 , and also between triangular flow v_3 and the triangularity of the IC ε_3 . Nevertheless, in all these studies fairly well-behaved (smooth) initial condition were used.

In this article we present a comparison between initial conditions and the anisotropic flow for very irregular (lumpy) initial conditions, for Au-Au collisions at 200 GeV. We also present a toy model, based on the One-Tube Model [3], in order to show why the eccentricity coefficients do not carry all the necessary information to understand the final momentum anisotropy.

2 Connection Between Flow and IC

In order to compare IC anisotropies with the azimuthal distribution of final-state hadrons we use the NeXSPheRIO code. This code is based on event-by-event 3+1D hydrodynamics, where the IC are generated by NeXuS, and SPheRIO solves the equations of relativistic

*E-mail: gardim@fma.if.usp.br

ideal hydrodynamics. The NeXSPheRIO code provides a good description for several experimental data trends, for instance, v_2 dependency on η and p_T , and v_2 fluctuations [4], directed flow v_1 [5], and reproduces the structure observed in two-particle correlations [6].

The analysis presented in this work was done for 1000 events equally divided into six centrality bins, and the hydrodynamics was computed for each event. Charged particles at mid-rapidity are used for the comparison. The anisotropic flow coefficients and reference angles come from the Fourier expansion of the azimuthal distribution of particles

$$v_n e^{in\Psi_n} \equiv \langle e^{in\phi} \rangle, \quad (1)$$

where ϕ is the azimuthal momentum angle. The eccentricity coefficients come from

$$\varepsilon_n e^{in\Phi_n} \equiv -\frac{\langle r^n e^{in\phi_s} \rangle}{\langle r^n \rangle}, \quad (2)$$

ϕ_s as spatial angle in the x-y plane. ε_n is computed in the C.M. system.

The comparison between average v_n and ε_n , as well as their fluctuations is shown in Fig. 1. For $n \geq 4$ the response to the average global initial geometry deformation, given by $\langle \varepsilon_n \rangle$, is not completely reflected in the flow coefficients. The average elliptic flow $\langle v_2 \rangle$ is proportional to the average ellipticity $\langle \varepsilon_2 \rangle$, except for $\varepsilon_2 \geq 0.6$, where the curve slope has a small deviation. As for $\langle v_1 \rangle$, it slightly increases with $\langle \varepsilon_1 \rangle$. The ratio $\langle v_1 \rangle / \langle \varepsilon_1 \rangle$ is not constant as already shown in Ref. [5]. For the average triangular flow, whose non-zero value is connected with the ridge effect [8], it is possible to observe two behaviors: for $\langle \varepsilon_3 \rangle < 0.4$ there is a direct relation between triangularity and triangular flow, positive and constant slope, however for $\langle \varepsilon_3 \rangle \geq 0.4$, $\langle v_3 \rangle$ decreases. In comparison to Refs. [1, 2], we have qualitatively the same result for $n = 2$, but somewhat different result for $n = 3$. Our $\langle v_3 \rangle / \langle \varepsilon_3 \rangle$ is not constant. Nevertheless an important result, in addition to the average values comparison, is the large dispersion values. Note that for lumpy IC, the eccentricity coefficients do not have all the information to understand the anisotropic flow. Since they give information about the global geometry, leaving aside the lumpiness of the IC.

Besides the connection between v_n and ε_n , it is important to compare the reference angles for IC Φ_n and flow Ψ_n , since it is expected that their mean values are equals. This comparison is plotted in Fig. 2. Due to the almond collisional shape of the IC, Ψ_2 is well correlated with Φ_2 . For $n = 3$, there is a correlation between the reference angle, but not as strong as for $n = 2$. However, for the other harmonics, the dispersions are larger.

3 Tube model for $\varepsilon_3=0$

The NeXSPheRIO results presented in Sec. 2 show that there is no strict event-by-event connection between v_n and ε_n . However, it is important to understand what features of the lumpy IC are manifested in final-state anisotropic flows. Inspired by the One-Tube Model [3], we create an IC with triangularity approximately equal to zero, and observe what happens with the triangular flow. The One-Tube Model provides an understanding of the ridge origin, and can be summarized as follows: NeXus IC conditions have tubular structures (along the collision axis). Using an IC composed of a smooth background energy

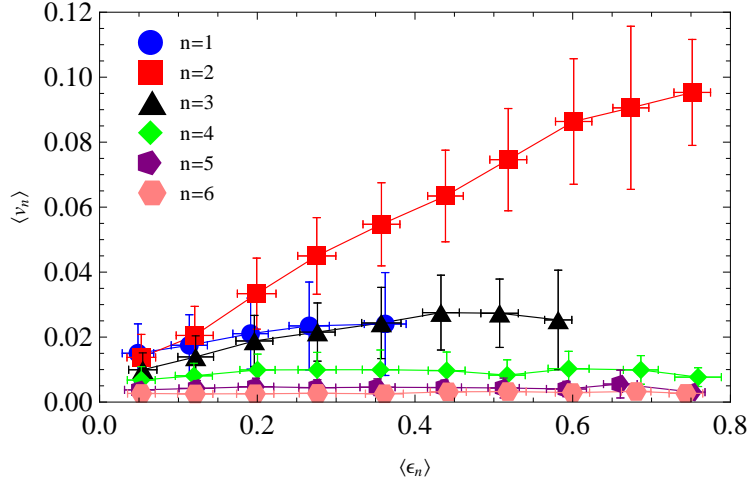


Figure 1: Comparison between v_n and ϵ_n for charged particles at mid-rapidity for Au-Au at 200 GeV.

density in the transverse plane plus one typical tube (for central collisions), we obtain two correlated peaks in the azimuthal distribution of particles. Due to this correlation, the 2-particle correlation has the 3 peak structure seen in the data [7]. However, for this correlation to appear, it is necessary that the tube be positioned near the boundary.

Keeping in mind the One-Tube model for central collisions, we compare three different IC. The first one is the One-Tube model, left plot in Fig. 3, with the triangularity $\epsilon_3^{(1t)} \simeq 0.067$. Then, we create an IC condition with three equal inner tubes, but with the same triangularity $\epsilon_3^{(3t)} \simeq 0.067$, center plot in Fig. 3. Finally, we consider an IC without triangularity $\epsilon_3^{(4t)} \simeq 0$, right plot Fig. 3. For these IC, we use a 2+1D version of the SPheRIO code, with longitudinal boost invariancy, to solve the ideal hydrodynamics.

The triangular flow obtained was: for the three inner tubes $v_3^{(3t)} \simeq 0.00095$, showing that the lumpiness in the internal region makes only a small contribution to the final anisotropy. However, for the ICs with the same peripheral tube, but with different inner region, almost the same value of the triangular flow was obtained: $v_3^{(1t)} \simeq 0.0110$ and $v_3^{(4t)} \simeq 0.0116$, respectively for the One-Tube case and $\epsilon_3 = 0$ case.

If one compares all the flow harmonics, it can be seen that for the IC with 3 inner tubes, not only v_3 is small, but all flow harmonics are closer to zero, leading to an almost isotropic distribution. For the other two ICs we conclude that the flow coefficients are almost the same, even though with different eccentricity coefficients. This result stresses the fact that there is no strict event-by-event relation between flow and eccentricity.

4 Conclusions

Using lumpy initial conditions for Au+Au at $\sqrt{s} = 200 \text{ AGeV}$ and solving hydrodynamics event-by-event, it was shown that $\langle v_n \rangle$ is not proportional to $\langle \epsilon_n \rangle$, except for the $n = 2$ case, which is dominated by geometry effects. In event-by-event hydrodynamics, there is no direct relation between v_n and ϵ_n , since the lumpiness is not completely captured by the eccentricity definition given by Eq. 2. Using NeXus and the Tube-Model IC, we

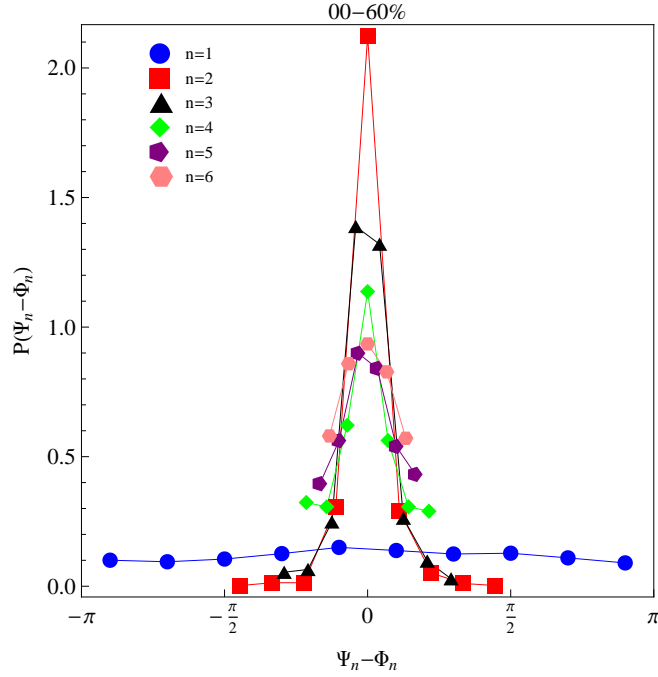


Figure 2: Comparison between Ψ_n and Φ_n for charged particles at mid-rapidity for Au-Au at 200 GeV. In abscissa axis is represented the difference $\Psi_n - \Phi_n$ and in the ordinate axis is plotted the probability density to get $\Psi_n - \Phi_n$.

understand that peripheral matter is more important than the inner matter for the momentum anisotropy in the final state at central collisions. This same behavior happens for peripheral collisions, but we cannot neglect the elliptic shape of initial overlap geometry as a significant contribution to anisotropic flow.

Acknowledgements

This work is funded by FAPESP under projects 09/16860-3 and 09/50180-0, and CNPq.

References

- [1] Z. Qiu, U. W. Heinz, Phys. Rev. **C84** (2011) 024911. [arXiv:1104.0650 [nucl-th]].
- [2] G. -Y. Qin, H. Petersen, S. A. Bass, B. Muller, Phys. Rev. **C82** (2010) 064903. [arXiv:1009.1847 [nucl-th]].
- [3] Y. Hama, R. P. G. Andrade, F. Grassi, W. -L. Qian, Nonlin. Phenom. Complex Syst. **12** (2009) 466-470. [arXiv:0911.0811 [hep-ph]].
- [4] Y. Hama, R. Peterson G. Andrade, F. Grassi, W. -L. Qian, T. Osada, C. E. Aguiar, T. Kodama, Phys. Atom. Nucl. **71** (2008) 1558-1564. [arXiv:0711.4544 [hep-ph]].
- [5] F. G. Gardim, F. Grassi, Y. Hama, M. Luzum, J. -Y. Ollitrault, Phys. Rev. **C83** (2011) 064901. [arXiv:1103.4605 [nucl-th]].

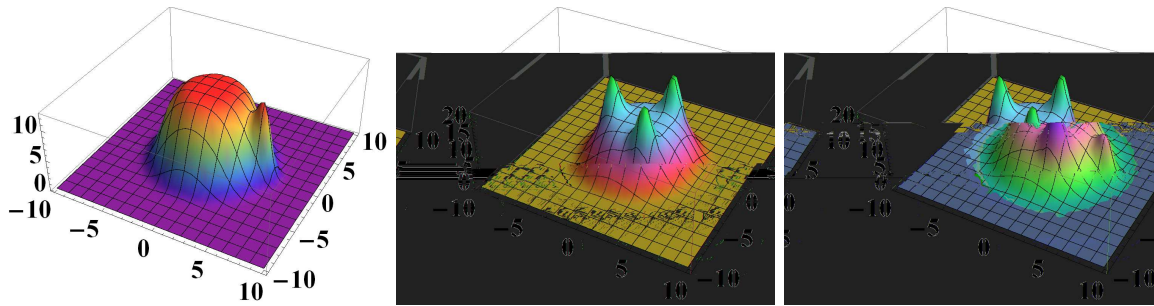


Figure 3: Energy density profiles for:(Left) One-Tube model, (center) 3 inner tubes, and (right) IC for $\varepsilon_3 = 0$.

- [6] J. Takahashi, B. M. Tavares, W. L. Qian, R. Andrade, F. Grassi, Y. Hama, T. Kodama, N. Xu, Phys. Rev. Lett. **103** (2009) 242301. [arXiv:0902.4870 [nucl-th]].
- [7] J. Putschke [STAR Collaboration], Nucl. Phys. **A783** (2007) 507-510.
- [8] B. Alver, G. Roland, Phys. Rev. **C81** (2010) 054905. [arXiv:1003.0194 [nucl-th]].